

Performance Analysis Of DSMST Converter FED BLDC Motor

^[1]Jeetender Vemula, ^[2]E. Vidya Sagar

^[1]Research Scholar,

Dept of EEE, Osmania University, Hyderabad, Telangana

^[2]Professor, Head

Dept of EEE, Osmania University, Hyderabad, Telangana

Abstract: A positive output voltage SEPIC-type DC-DC converter called DSMST (modified SEPIC topology) without a transformer for use in electric vehicles. The DSMST converter is derived from the traditional SEPIC converter with the addition of a switching cell. Furthermore, the output diode and inductors are interchanged for the continuous output current. In the realm of electric vehicles, the utilization of Brushless DC (BLDC) motor drives coupled with a DC-DC converter has become increasingly important. Specifically in the context of electric vehicles, the use of BLDC motors offers several technical advantages compared to other types of motors such as DC, induction, and switched reluctance motors. The DSMST converter is connected to the BLDC motor through a three-phase voltage source inverter (VSI) to regulate the voltage and current supplied to the BLDC motor, ensuring optimal performance. To regulate the speed of drive, a closed loop control system is developed using hall sensor signals. The proposed system is developed in the MATLAB/Simulink to check the applicability of electric vehicle configuration and the results shown that the proposed converter is well suitable for electric vehicle applications.

Keywords: DC-DC Converter, BLDC Motor, Electric vehicle

1. Introduction

In their article from 1991, Pillay and Krishnan spoke about the differences between BLDC motors and PMSM. Assuming that both the BLDC and the PMSM are functioning in the mode of operation that maintains a constant torque, the BLDC has a greater torque per unit peak current than the PMSM. When compared with the PMSM, the BLDC has the potential for a greater power density. As a result, the BLDC should be favoured over the PMSM in situations where there is a limitation on either weight or space.

As people become increasingly concerned about their impact on the environment, electric cars are gaining in popularity. When the electrical components of electric cars are taken into consideration, there are three primary areas: the battery charging system, the battery management system, and the motor drive systems. When it comes to the motor drive system for medium and low power electric cars, PM BLDC motors are employed in the system the majority of the time. When compared to other motors of the same size that are now available, PM BLDC motors are capable of having a better power density and generating the most torque per ampere that is possible. In particular, the performance of these motors is outstanding and has been shown to be great for the servo application and the traction application, both of which need the drive to function in the zone of constant torque. PM BLDC motor drive design necessitates parameter estimate of the motor for the purpose of motor control, the fundamental functioning of the motor achieved by the combination of hall sensors, and the accurate designing of tuned control parameter based on the motor's parameters. In this chapter, a step-by-step approach for monitoring PM BLDC motor parameters is presented in detail for the first time. Following that, the hall combination that is used for the excitation of the motor phases of an experimental motor is detailed, and then the open-loop response for the same motor is shown.

To get around problems with power quality, DC-DC converters and BLDC motors are often used together. Electronic switching-mode DC to DC converters take an input of one DC voltage level and output a different DC voltage level. This is accomplished by briefly storing the energy from the input and then releasing it to produce the output voltage at a different level. It has been proved by Ping et al. (2010) that the output voltage is controlled throughout a large battery lifespan, and that the output ripple is reduced when the mode is being transitioned.

When the voltage from the battery drops, the converter has the ability to switch between the boost, buck-boost, and buck modes. Because the DC-DC converter may operate in a variety of modes, it is necessary to ensure that the system is stable, that there is little ripple in the output voltage, and that the regulated output voltage is accurate during mode transition 24. Tingna Shi et al. (2010) has provided an illustration concerning, a unique topology of a circuit, in which an adequate DC link voltage is employed to drive phase currents to grow and drop in the similar slope. This results in a significant reduction of pulsated commutation torque.

Mohammed Fazil and colleagues (2010) have accomplished the task of lowering the cogging torque across tapered air-gap profiles in their research. In their study, Chen et al. (2013) spoke about the several kinds of DC-DC converters that are accessible for the input control circuit. Some of the most fundamental kinds of circuits for DC-DC converters. (Chen et al. 2014) describe four different types of converters: fly back, buck, boost, and buck-boost. A buck boost converter fed brushless DC motor drive with variable DC link voltage of VSI was presented by Vashist Bist et al. (2014). This drive improves power quality at AC mains while reducing the number of components required. Yu Chen et al. (2014) has presented and suggested the new architecture that includes a buck power factor correction and buck DC-DC cells. Because this new topology results in a low voltage stress across the DC link capacitor, electrolytic capacitors that have a low voltage rating, but a big capacity may be employed. The high step-down from the input voltage to the output voltage is achieved by integrating two buck cells.

A strategy for controlling the speed of a sensor less Brushless DC motor by monitoring the back EMF has been developed and implemented by Kavitha et al. (2015). A bridgeless buck boost converter fed brushless DC motor drive that improves total harmonic distortion has been developed by Gaurav Gupta and his colleagues (2015). This drive is intended for low power applications. The power factor correction based bridgeless Luo converter fed brushless DC motor drive has been experienced by Bhim Singh et al. (2015).

Yoon and Kim (2018) devised a plan for the creation of a precise control for a sensor less brushless direct current (BLDC) motor that utilizes a permanent magnet. The control technique used in this design is operating well thanks to the Phase Lock Loop (PLL). The functioning of this design is dependent on the third harmonic signals. Within the framework of the developed permanent magnet BLDC motor, the commutation instances of the motor's internal voltage from the third harmonic are employed. The fundamental and higher order harmonics are present in this waveform. The stator phase voltage is used to derive the third harmonic of the oscillator. This stator phase voltage harmonic 26 signal is responsible for maintaining rotor flux with a steady phase relation over the whole speed and load situation spectrum. Because it is not susceptible to any of the filtering delays, the motor can now achieve high performance over a wide variety of speed ranges thanks to the step that was just presented. The comparison between the suggested system and the permanent magnet BLDC motor reveals that the proposed system has a straightforward hardware design, is capable of functioning throughout a broad speed range, and comes at a reasonable price.

Input Output Place Transition (IOPT) flow modelling framework has been given by Pereira and Gomes (2017). This framework includes a series of tools such as graphical editors, simulators, and auto code generators to construct the controller implementation. With the help of the FPGA kit, we were able to construct this implementation-based prototype of a servo motor controller. A SPARTAN 3E 1600 FPGA board-based controller that uses the Model based Predictive regulate (MPC) method has been suggested by Darba et al. (2016). This controller would be used to regulate the stator current and rotor speed of BLDC machines.

2. Brushless DC Motor (BLDC):

The use of permanent magnets in electrical machines rather of electromagnetic excitation leads in a number of benefits, including the elimination of losses caused by excitation, simplification of design, enhanced efficiency, rapid dynamic performance, and high torque or power per unit volume. Because of the low quality of PM materials available in the early 19th century, the PM excitation was not used at that time. The development of alnico in 1932 rekindled interest in the usage of PM excitation systems; nevertheless, since then, their use has been restricted to dc commutator machines with fractional or very low horsepower [18].

The term "brushless direct current" (BLDC) refers to a synchronous electric motor that is powered by direct-current electricity (DC) and that features a commutation system that is electronically controlled, as opposed to a mechanical commutation system that is based on brushes. This kind of motor is known as a

"brushless direct current" (BLDC) motor. Brushless direct current (BLDC) motors are another name for this specific kind of electric motor. The correlations between current and torque, voltage and rpm are all linear in these sorts of motors. In a brushless direct current (BLDC) motor, the electromagnets do not spin; rather, the permanent magnets do, and the armature does not move at all.

This is in contrast to a traditional AC motor, in which the electromagnets spin. By acting in this manner, we sidestep the problem of figuring out how to provide current to an armature that is moving. In order to do this, the brush systems assembly must first be removed before making way for the installation of an electronic controller. The controller is very much like the commutator and brushes that are used in brush DC motors; but, in place of those components, it makes use of a static solid-state circuit in order to accomplish the identical task of power distribution.

3. Hall Effect Sensors:

A Hall Effect Sensor is a sensor that is often used to give feedback on the position of the rotor to a motor controller. Let's have a better understanding of the role that this sensor plays in the motor control system of an automobile. A BLDC motor control system is a complex circuit that consists of multiple components working in conjunction with one another to cause the motor to operate in the way that is intended.

When constructing this kind of system, the most important factors for the engineers to consider are how efficient it is, how long it will last, and how well it will perform. A microprocessor serves as the motor's "brain," while the magnets and coils are responsible for the electrical component of the motor's operation. However, even the most sophisticated brain need information from the senses. In this context, the two sensory inputs that are given a great deal of weight are speed and position. Let's get a grasp on them within the framework of the motor vehicle industry. The significance of using a hall-effect sensor in a motor controller application for an automobile will be shown with the help of the following example.

Electric power steering (EPS) systems are a good example of the significant role that Hall Effect sensors play in the development of motor control solutions for automobiles. When a vehicle is equipped with an electronic power steering (EPS) system, the steering wheel is turned by the driver with the assistance of a tiny electric motor, which makes it much simpler to control the vehicle at moderate speeds.

Hall Effect sensors are used to determine the position of both the steering wheel and the rotor of the electric motor. This helps to guarantee accurate control of the electric motor. The motor controller receives data from these sensors, and it uses that information to modify the amount of power that is given to the motor in response to the inputs provided by the driver as well as the position of the steering wheel. Because the motor controller would not be able to precisely calculate the location of the steering wheel or the rotor in the absence of Hall Effect sensors, the vehicle might become unstable or unpredictable.

3.1 Importance of Speed and Position of the Rotor in Motor Commutation:

Commutation in a BLDC motor is a process that takes place over the course of 6 steps. A three-phase H-bridge is used to produce six flow vectors, each of which causes the motor to rotate by 60 degrees (corresponding to the next position), for a total of 360 degrees of rotation. This completes one revolution of the motor. A current is sent to the stator's coil by the motor controller so that the motor may rotate. This results in the generation of a magnetic field, which then generates torque on the rotor (which is a permanent magnet). As a direct consequence of this, the rotor begins to rotate. Now, because of the switch in polarity, the rotor will tend to come to a halt if it gets close to the magnetic field that is driving it when it reaches this point. At this point, the magnetic field will start to attract the rotor, which will cause the movement to come to an abrupt halt. In order to prevent this from happening, the motor control system will alter the current that is delivered to the stator. This will result in the creation of a new magnetic field, which will allow the rotor to continue rotating. Therefore, switching the current at the appropriate time is the most important part of the commutation process. As a result of the necessity to identify the "right instance" as soon as it occurs, the concepts of speed and location become relevant to the situation.

It is necessary to have a sensor in order to provide input to the system that controls the motor and indicate when the rotor has arrived at the appropriate position. If the commutation is carried out at a rate that is either faster or slower than the speed of the rotor, the magnets will go out of phase with the magnetic field

produced by the stator. Because of this, the rotor will begin vibrating and will eventually come to a halt. Following the completion of one cycle of commutation, it is necessary to ascertain the location of the rotor in relation to the stator in order to start the subsequent cycle of commutation. And as a result, the identification of the location is also an essential component.

The electric motor business makes use of several different kinds of sensors, including encoders, switches, and potentiometers, amongst others. However, the Hall Effect Sensor is now the sensor that has the greatest number of applications and deployments. In the following paragraphs, we will go into further depth about the Hall Effect Sensor and the function that it serves in a motor control system.

3.2 Working of Hall Effect Sensors:

A BLDC motor will, in most cases, have three Hall Effect Sensors installed on either the rotor or the stator of the motor. These Hall sensors are separated by 120 degrees from one another, which provides a position range of 0 to 360 degrees for the angle. These hall sensors will produce a corresponding digital pulse in terms of 1 and 0 when they come into contact with the magnetic field of the rotor, as seen in the fig that can be found below. These hall sensors are capable of determining the motor position (Angle) in a total of six stages. The rectangular waveforms in the fig illustrate the positive and the negative pulse created at the appropriate angle by each of the three Hall Effect Sensors (A, B, and C). These pulses are shown in the positive and negative directions, respectively.

The explanation that follows will bring about greater comprehension. When a rotor magnet passes through one of the sensors, that sensor will either emit a low signal or a high signal, depending on whether the North Pole or the South Pole of the rotor has been traversed by the magnet. Because each of the three sensors alternates between a low and high state as the rotor passes in front of it, the location of the rotor can be determined precisely every 60 degrees.

The Hall-effect Sensor is able to discern between a positive charge and a negative charge that are moving in the opposite direction. Both charges are moving in the same general direction. The hall-effect sensor will convert the magnetic field that it detects into a suitable analog or digital signal for the electronic system, which is often a motor control system. This will allow the magnetic field to be read by the electronic system.

The truth table that was derived from the readings of the three Hall Effect Sensors may be seen shown further down the page, as indicated in the previous sentence. As can be seen, the signal that is obtained from the sensor is what controls the state that each transistor in the H-Bridge is in. This state is dictated by the signal. The movement in the counter clockwise direction (CCW) is indicated by the arrow pointing above, while the movement in the clockwise direction (CW) is represented by the arrow pointing downwards.

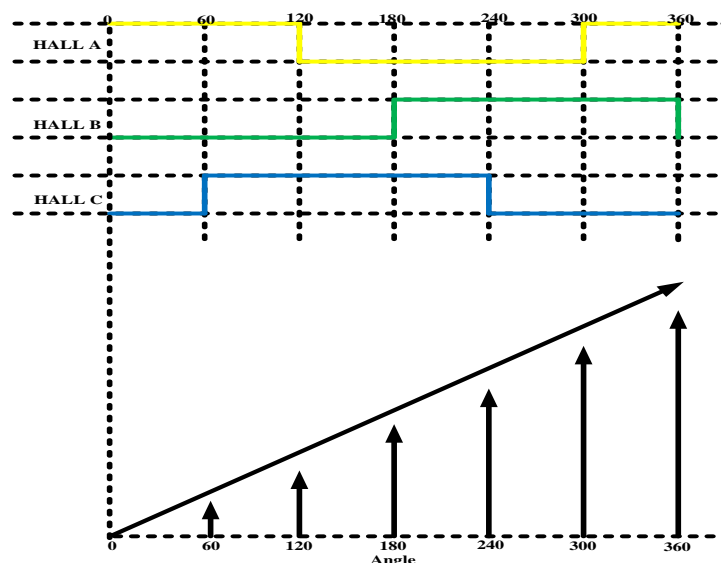


Fig 1: Corresponding graph also illustrates how one commutation is completed in 6 steps as the angle reached 360 degrees.

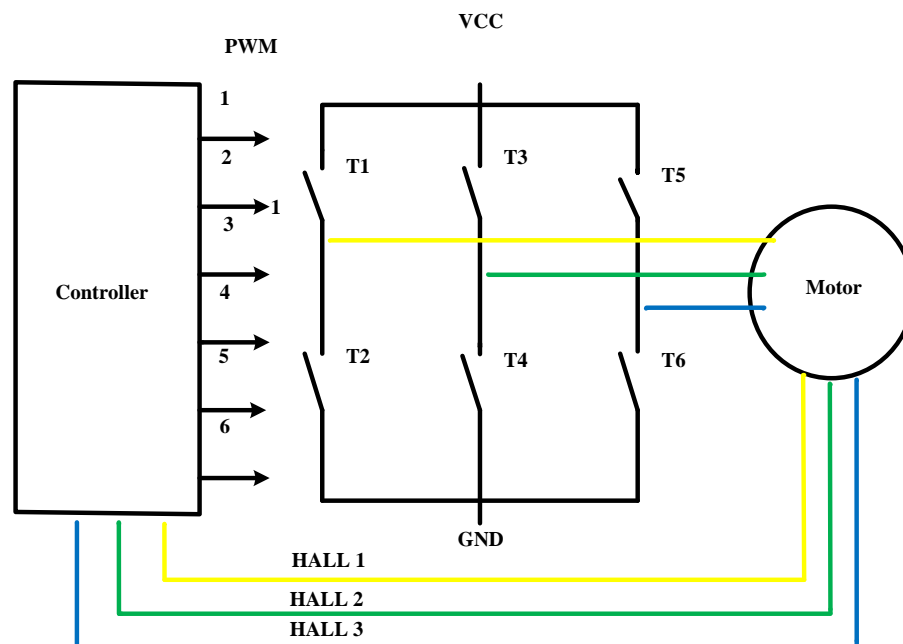


Fig 2: The diagram below shows a typical BLDC Motor Controller. Three lines going from the motor to the controller depict the signal sent by the three Hall Effect Sensors.

Table 1: Truth Table of Hall signals A, B, C and Transistor states.

HALL A	HALL B	HALL C	TRANSISTOR STATE	
1	0	0	T3	T2
1	0	1	T3	T6
0	0	1	T1	T6
0	1	1	T1	T4
0	1	0	T5	T4
1	1	0	T5	T2

- Calculation of the Angle: This is done based on the signal from the Hall Effect Sensor, which can be seen in fig 2. An estimated angle between 0 and 360 degrees is determined by the pulse from the Hall sensor.
- Calculation of Speed: The calculation of speed involves computing the periods of the signal produced by the Hall Effect Sensor. Calculating period, frequency, and speed according to the following formula requires the use of the term period. The equation for frequency = 1/period.

Only one hall sensor is enough for calculating the speed.

4. Improving EV Performance with Hall-effect Sensors:

Although electric motors are used to power auxiliary systems in internal combustion engines, such as anti-lock brakes and power windows, the powertrain of electric cars is truly driven by motors. Because of the direct relationship between the hall-effect sensors' accuracy and the operation of the electric car, the relevance of this situation lends itself to an even higher degree of importance for the sensors.

The introduction of Hall Effect sensors into electric automobiles makes it possible for highly precise monitoring and control of the speed and position of the motor, which in turn allows the vehicle to offer

performance that is both efficient and reliable. This is because the sensors make it possible to monitor and control the speed at which the motor is spinning as well as its position. For example, the sensor makes it possible for the car to accurately alter the torque output of the motor, which is essential for the continued operation of the vehicle's stability and traction control systems.

Additionally, the Hall Effect sensor is used in some capacity by the regenerative braking system, which is an important component of electric vehicles and is used in some capacity by electric vehicles. They are able to recoup the energy that is lost as a result of braking and save it in the battery so that it may be used at a later time. This not only improves the vehicle's overall energy efficiency but also extends its range, which is the primary differentiating factor among the various types of electric vehicles.

Additionally, the Hall Effect sensor is another component that adds to the overall safety of electric automobiles and is an important part of the electric vehicle. Due to the fact that it monitors the position of the wheels in addition to the other components, the sensor is able to determine whether or not there are any potential issues or failures in the system. It is possible that the driver will be given early warning, and necessary actions will be able to be performed, all with the intention of preventing accidents and reducing the amount of damage done to the vehicle.

5. BLDC MODELLING

The development of a mathematical model for a Brushless DC (BLDC) motor can be approached in a manner similar to that used for a three-phase synchronous machine. Due to the permanent magnet installed on its rotor, certain dynamic features of the system exhibit variations. The flux linkage originating from the rotor is contingent upon the magnet. Hence, the phenomenon of magnetic flux linkage saturation is commonly observed in motors of this nature. Similar to conventional three-phase motors, the design of a brushless DC (BLDC) motor is powered by a three-phase voltage source. The source does not necessarily need to exhibit sinusoidal behaviour. A square wave or any other waveform can be utilized as long as the peak voltage remains within the motor's maximum voltage limit. In a similar vein, the representation of the armature winding for the brushless DC (BLDC) motor can be formulated as follows.

$$V_a = R i_a + L \frac{di_a}{dt} + e_a \quad (1)$$

$$V_b = R i_b + L \frac{di_b}{dt} + e_b \quad (2)$$

$$V_c = R i_c + L \frac{di_c}{dt} + e_c \quad (3)$$

Can also be rewritten in matrix as,

$$\begin{bmatrix} v_a \\ v_b \\ v_c \end{bmatrix} = \begin{bmatrix} R + pL & 0 & 0 \\ 0 & R + pL & 0 \\ 0 & 0 & R + pL \end{bmatrix} \begin{bmatrix} i_a \\ i_b \\ i_c \end{bmatrix} + \begin{bmatrix} e_a \\ e_b \\ e_c \end{bmatrix}$$

Where $L_a = L_b = L_c = L = L_s - M$

M=multiplying inductance

v_a, v_b, v_c = terminal phase voltage in volts

e_a, e_b, e_c = motor back EMF in volts

i_a, i_b, i_c = motor input current in amperes

L_a =armature of self-inductance

$R_a = R_b = R_c = R$ = armature resistance in ohm

P in the matrix represent $\frac{d}{dt}$

The trapezoidal shape of the back electromotive force (EMF) of the rotor can be attributed to the presence of a permanent magnet. The formulation of the back electromotive force (EMF) needs to be adjusted as articulated in

$$e_a(t) = K_E * \phi(\theta) * \omega(t) \quad (4)$$

$$e_b(t) = K_E * \phi\left(\theta - \frac{2\pi}{3}\right) * \omega(t) \quad (5)$$

$$e_c(t) = K_E * \phi \left(\theta + \frac{2\pi}{3} \right) * \omega(t) \quad (6)$$

Where ω is running speed of the motor and K_E is the back EMF constant.

The trapezoidal flux linkage is likewise influenced by the permanent magnet, resulting in the production of torques. Considering the torque constant, denoted as K_T . The torques that were generated.

$$T_E = \frac{e_a i_a + e_b i_b + e_c i_c}{\omega} \quad (7)$$

The final torque, T_E , can be attained by the subsequent expressions.

$$T_a(t) = K_T * \phi(\theta) * i_a(t) \quad (8)$$

$$T_b(t) = K_T * \phi \left(\theta - \frac{2\pi}{3} \right) * i_b(t) \quad (9)$$

$$T_c(t) = K_T * \phi \left(\theta + \frac{2\pi}{3} \right) * i_c(t) \quad (10)$$

$$T_E(t) = T_a(t) + T_b(t) + T_c(t) \quad (11)$$

The angular motion of the rotor can be expressed using Newton's second law of motion.

$$T_E(t) - T_L(t) = J \frac{d\omega(t)}{dt} + B * \omega(t) \quad (12)$$

Where,

J rotor inertia in $[\text{kg/m}^2]$,

T_L load torque is in N-m, B damping constant.

6. Results & Discussion:

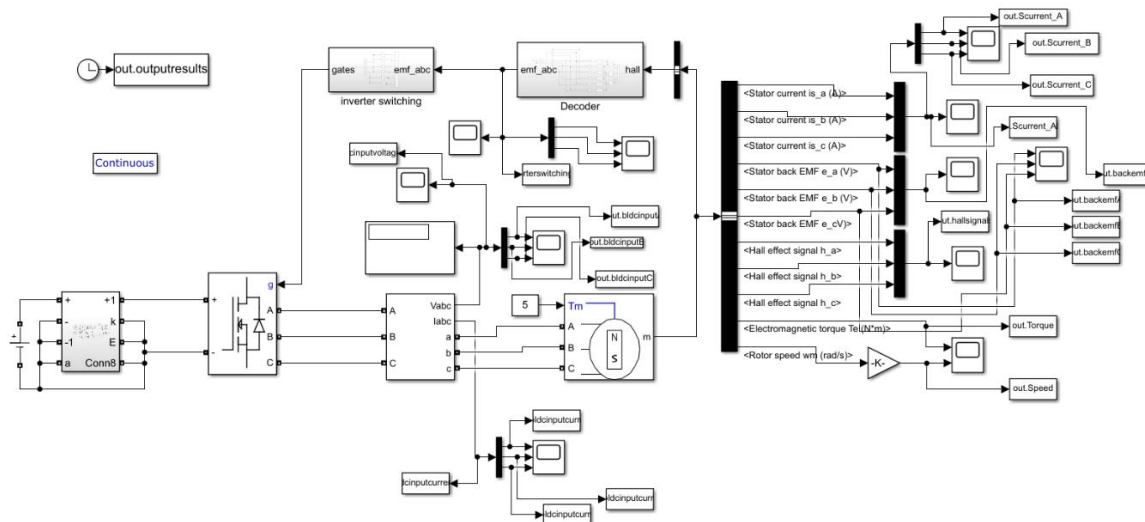


Fig 3: Simulink diagram of dc-to-dc converter driving BLDC motor by VSI control

The Fig. 3 shows the Simulink diagram of closed loop dc-dc converter which has all the with respect to the MATLAB software such as permanent magnet synchronous motor acting as BLDC motor, three phase VSI, scopes for viewing results, workspace blocks which are used to carry the obtained result or output the workspace of command window so that results can be extracted there, displays, summer, step input signal etc,...

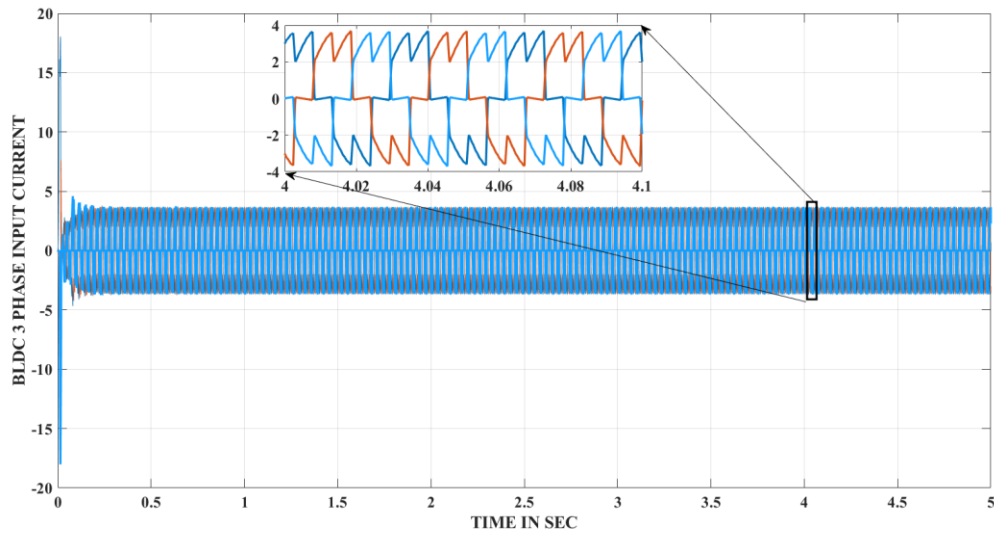


Fig 4: Three Phase BLDC input current

Fig 4. The above waveform shows regarding 3 phase input current given to the BLDC motor between 0 to 5 seconds time interval. The magnitude of input current of each phase is predominantly at 4 amps i.e., these currents are altering between -4 to +4 amps. These currents reached to steady state in less than 0.25 seconds.

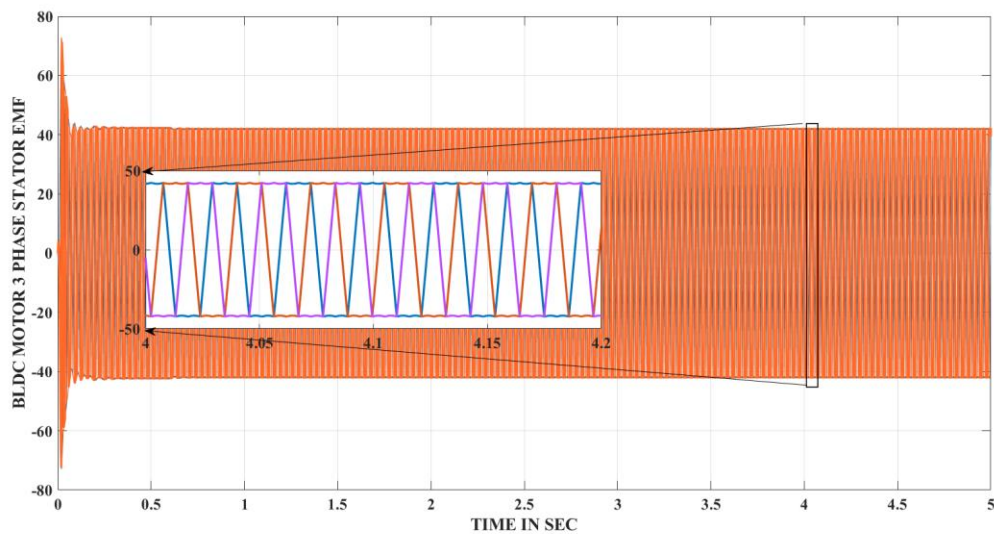


Fig 5: Three Phase BLDC stator voltage

Fig 5. The above waveform shows regarding 3 phase stator EMF given to the BLDC motor between 0 to 5 seconds time interval. The magnitude of input current of each phase is predominantly at 40 i.e., these currents are altering between -40 to +40. This EMF reached to steady state in less than 0.25 seconds.

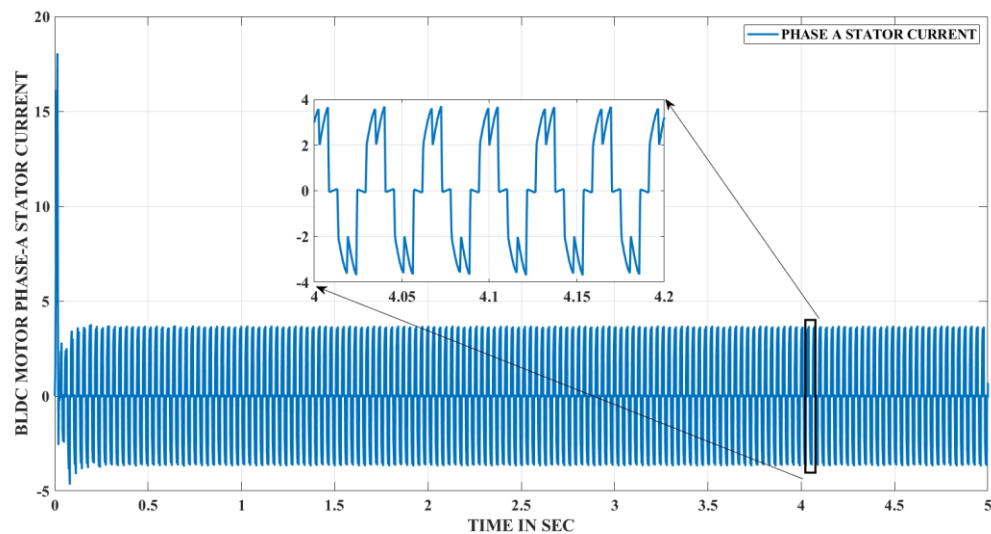


Fig 6: Phase-A BLDC stator current

Fig 6 The above waveform shows regarding 3 phase-A stator current given to the BLDC motor between 0 to 5 seconds time interval. The magnitude of phase-A stator current of each phase is predominantly at 4 amps i.e., these currents are altering between -4 to +4 amps. These currents reached to steady state in less than 0.25 seconds.

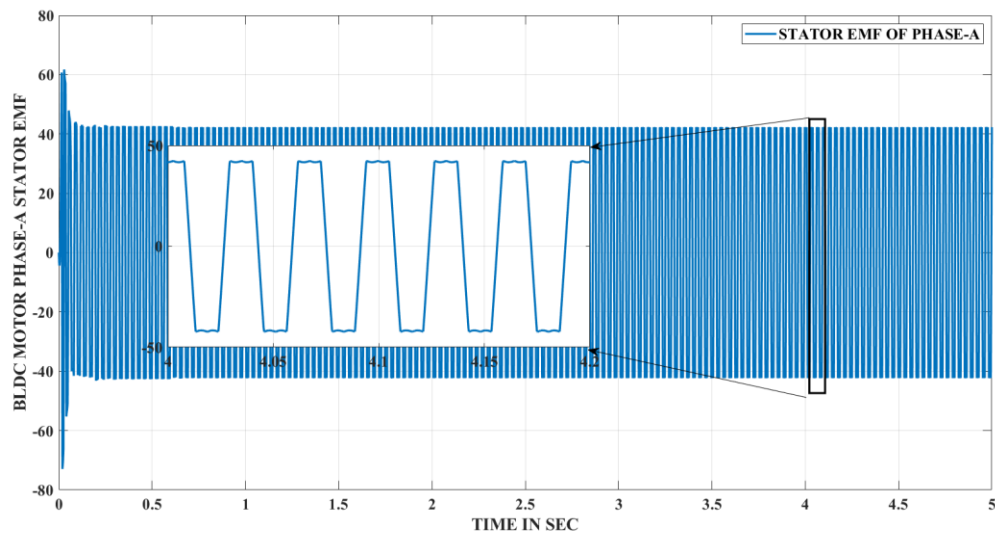


Fig 7: Phase-A BLDC stator emf

Fig 7 The above waveform shows regarding 3 phase-A stator EMF given to the BLDC motor between 0 to 5 seconds time interval. The magnitude of input current of each phase is predominantly at 40 i.e., these currents are altering between -40 to +40. This EMF reached to steady state in less than 0.25 seconds.

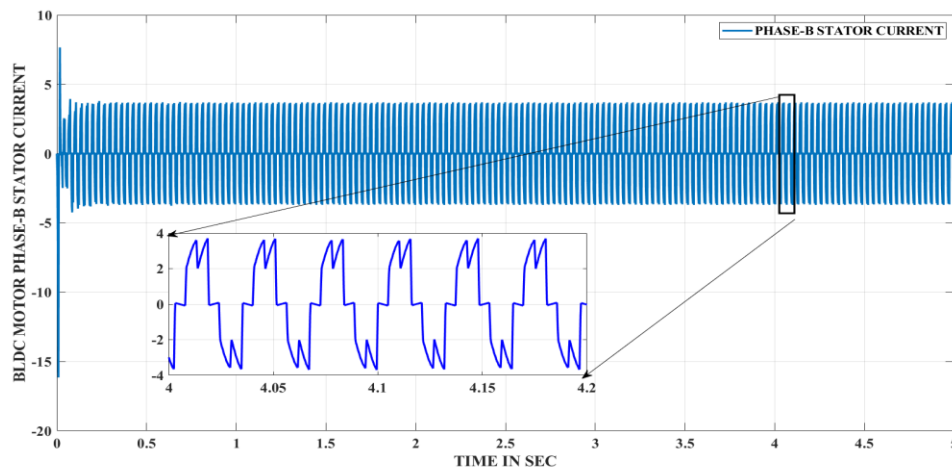


Fig 8: Phase-B BLDC Stator Current

Fig 8 The above waveform shows regarding 3 phase-B stator current given to the BLDC motor between 0 to 5 seconds time interval. The magnitude of phase-A stator current of each phase is predominantly at 4 amps i.e., these currents are altering between -4 to +4 amps. These currents reached to steady state in less than 0.25 seconds.

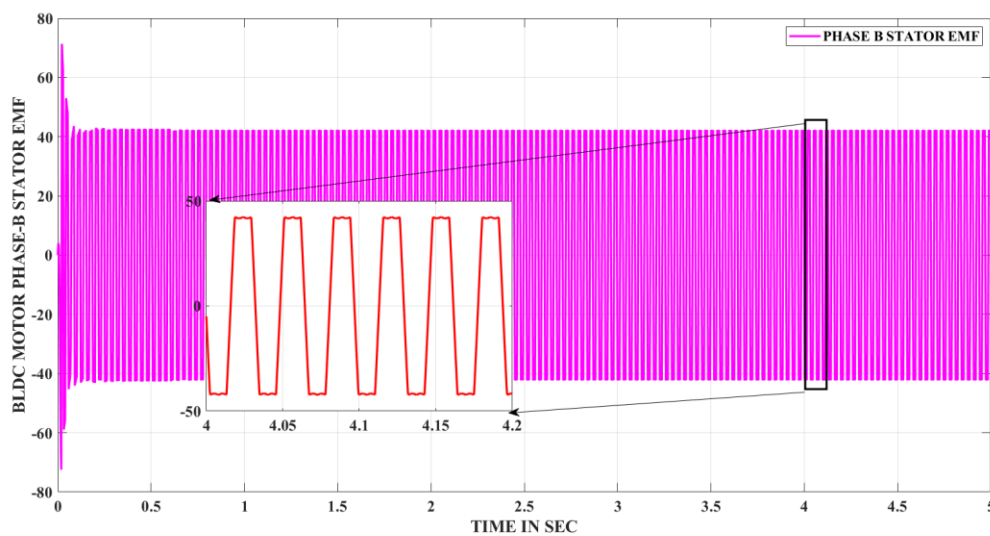


Fig 9: Phase-B BLDC Stator Emf

Fig 9 The above waveform shows regarding 3 phase-B stator EMF given to the BLDC motor between 0 to 5 seconds time interval. The magnitude of input current of each phase is predominantly at 40 i.e., these currents are altering between -40 to +40. This EMF reached to steady state in less than 0.25 seconds.

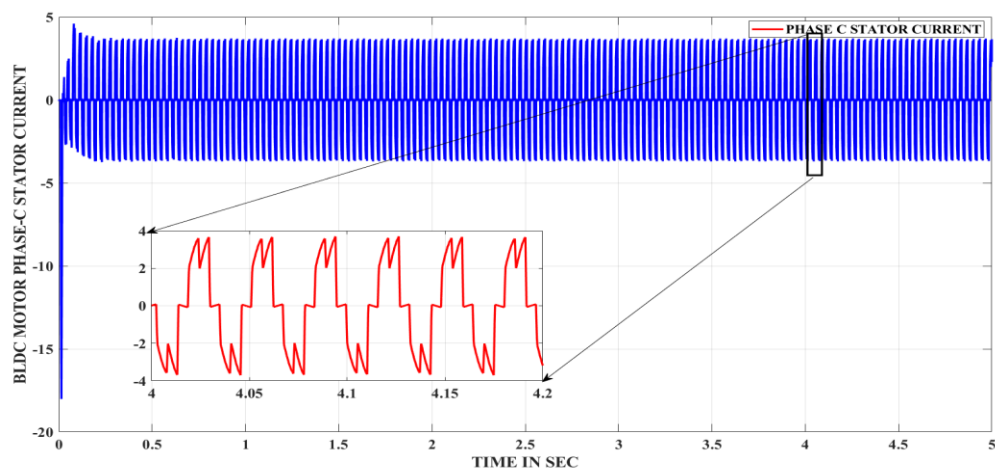


Fig 10: Phase-C BLDC Stator Current

Fig 10 The above waveform shows regarding 3 phase-C stator current given to the BLDC motor between 0 to 5 seconds time interval. The magnitude of phase-A stator current of each phase is predominantly at 4 amps i.e., these currents are altering between -4 to +4 amps. These currents reached to steady state in less than 0.25 seconds.

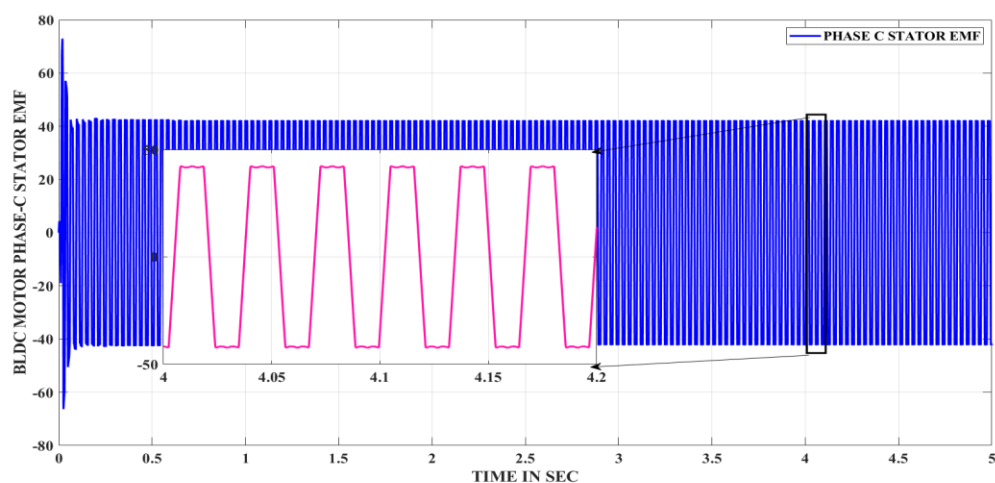


Fig 11: Phase-B BLDC Stator EMF

Fig 11 The above waveform shows regarding 3 phase-C stator EMF given to the BLDC motor between 0 to 5 seconds time interval. The magnitude of input current of each phase is predominantly at 40 i.e., these currents are altering between -40 to +40. This EMF reached to steady state in less than 0.25 seconds.

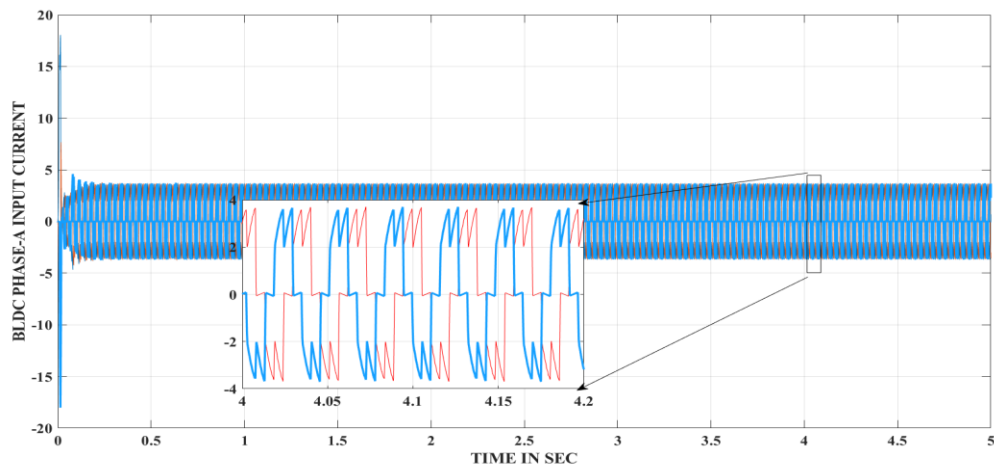


Fig 12: phase-A BLDC input current

Fig 12 The above waveform shows regarding 3 phase-A input current given to the BLDC motor between 0 to 5 seconds time interval. The magnitude of input current of each phase is predominantly at 4 amps i.e., these currents are altering between -4 to +4 amps. These currents reached to steady state in less than 0.25 seconds.

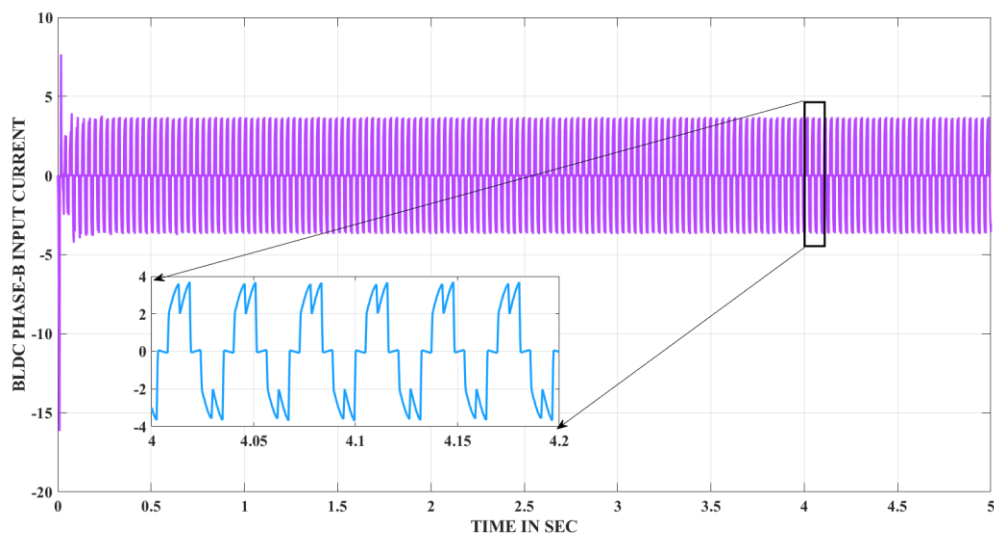


Fig 13: phase-B BLDC input current

Fig 13 The above waveform shows regarding 3 phase-B input current given to the BLDC motor between 0 to 5 seconds time interval. The magnitude of input current of each phase is predominantly at 4 amps i.e., these currents are altering between -4 to +4 amps. These currents reached to steady state in less than 0.25 seconds.

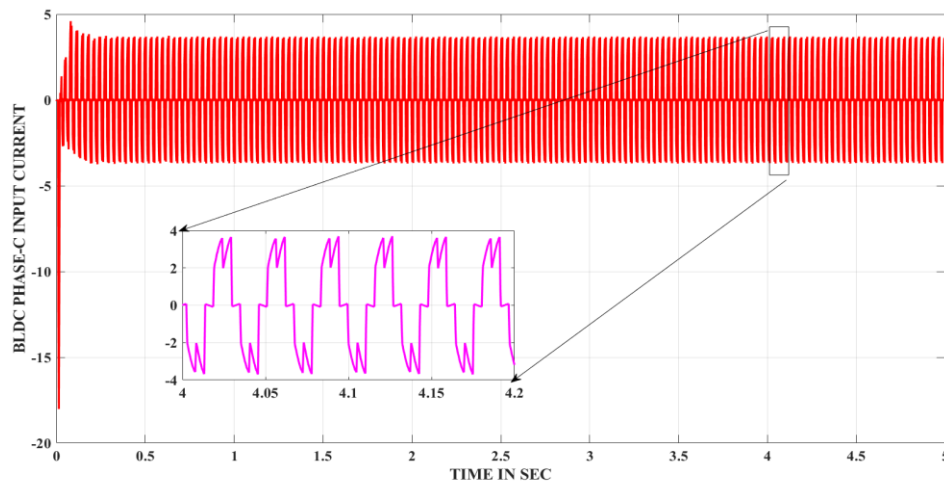


Fig 14: phase-B BLDC input current

Fig 14 The above waveform shows regarding 3 phase-C input current given to the BLDC motor between 0 to 5 seconds time interval. The magnitude of input current of each phase is predominantly at 4 amps i.e., these currents are altering between -4 to +4 amps. These currents reached to steady state in less than 0.25 seconds.

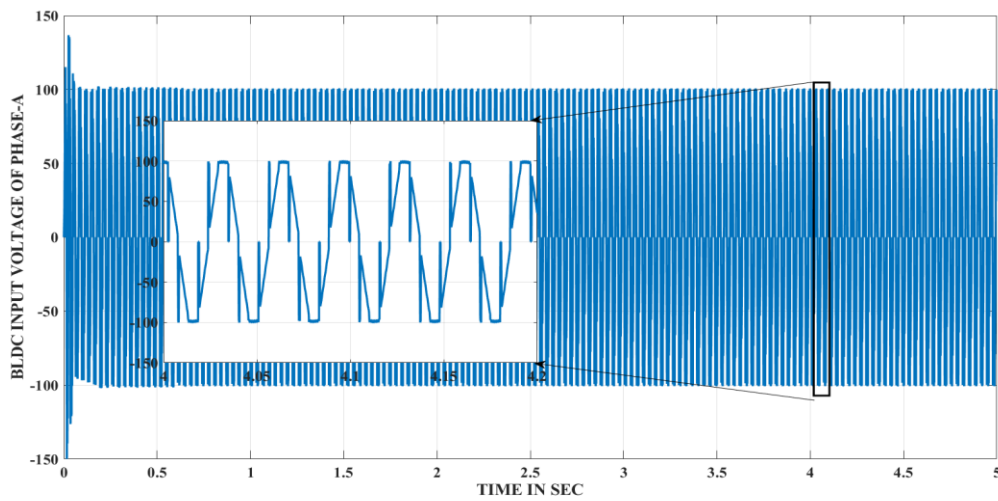


Fig 15: Phase-A BLDC input Voltage

In Fig 15 the above waveform shows regarding 3 phase-A input voltage given to the BLDC motor between 0 to 5 seconds time interval. The magnitude of input voltage of each phase is predominantly at 100V i.e., these currents are altering between -100 to +100 Volts. This voltage reached to steady state in less than 0.25 seconds.

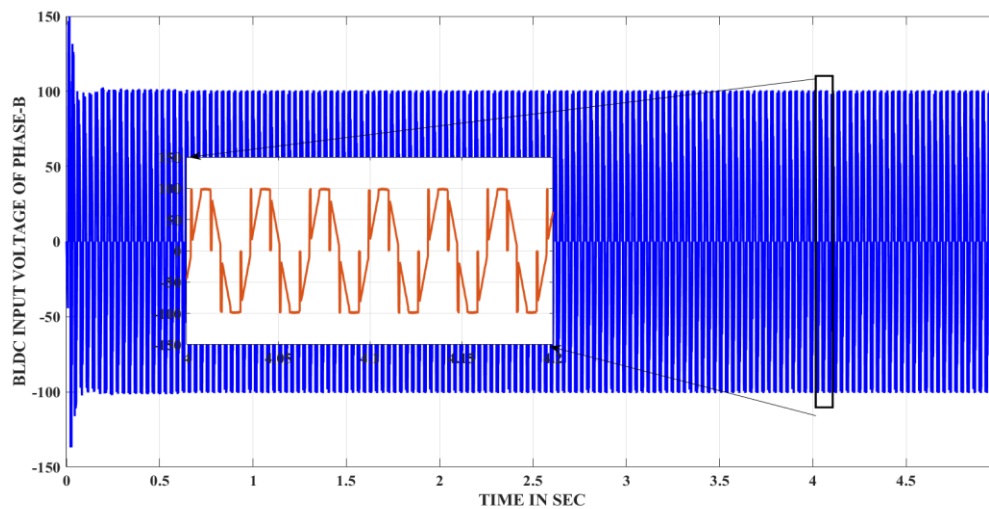


Fig 16: Phase-B BLDC input Voltage

Fig 16 The above waveform shows regarding 3 phase-B input voltage given to the BLDC motor between 0 to 5 seconds time interval. The magnitude of input voltage of each phase is predominantly at 100V i.e., these currents are altering between -100 to +100 Volts. This voltage reached to steady state in less than 0.25 seconds.

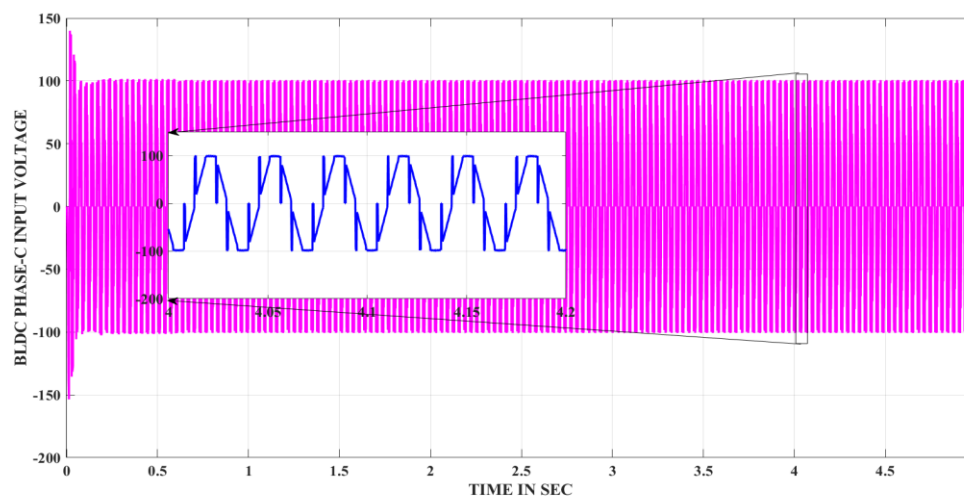


Fig 17: Phase-C BLDC input Voltage

Fig 17 The above waveform shows regarding 3 phase-C input voltage given to the BLDC motor between 0 to 5 seconds time interval. The magnitude of input voltage of each phase is predominantly at 100V i.e., these currents are altering between -100 to +100 Volts. This voltage reached to steady state in less than 0.25 seconds.

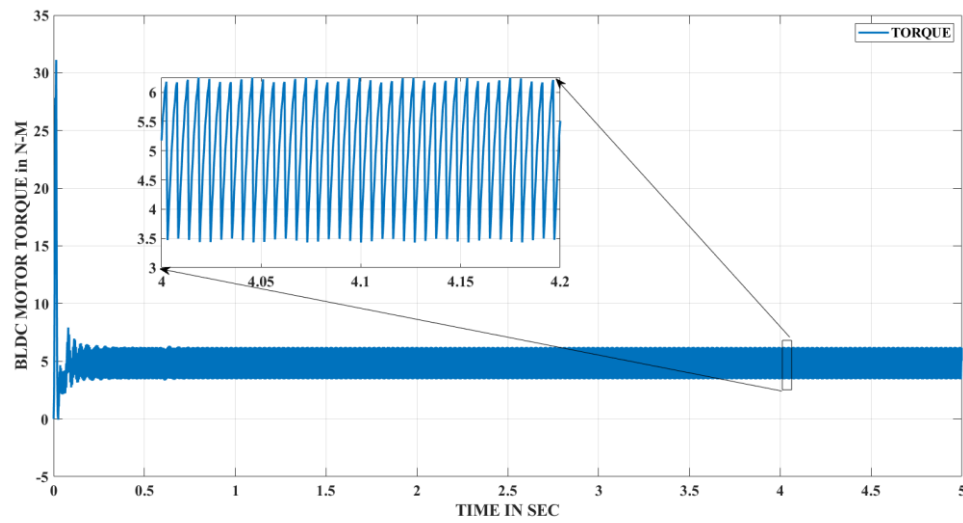


Fig 18: BLDC Motor Torque

Fig 18 the above waveform shows regarding torque given to the BLDC motor between 0 to 5 seconds time interval. The magnitude of input voltage of each phase is at 5N-M. This torque reached to steady state in less than 0.25 seconds.

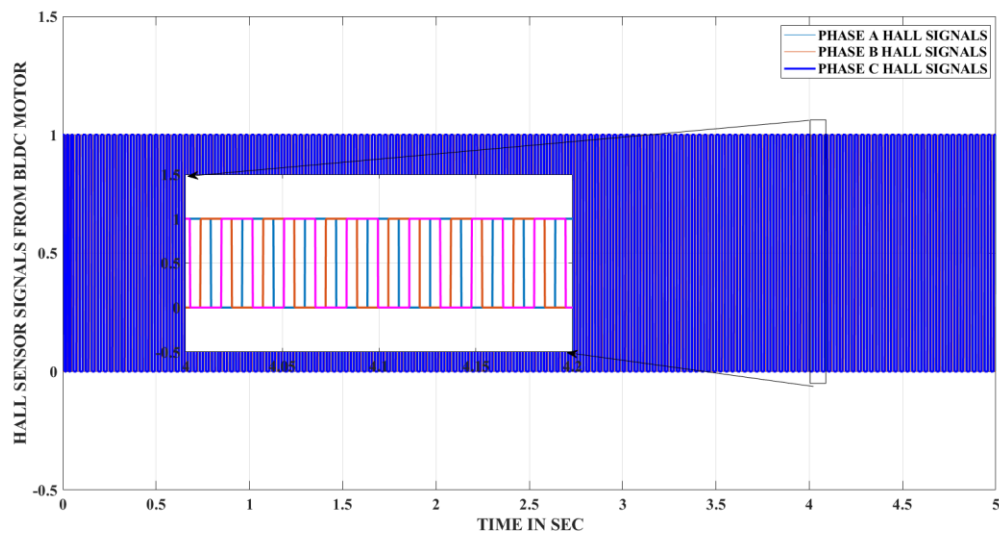


Fig 19 BLDC Motor Hall Sensor Signals

Fig 19 the above waveform shows regarding Hall signals of phase-A, phase-B, phase-C given to the BLDC motor between 0 to 5 seconds time interval. The magnitude of Hall signals of each phase is at 1.

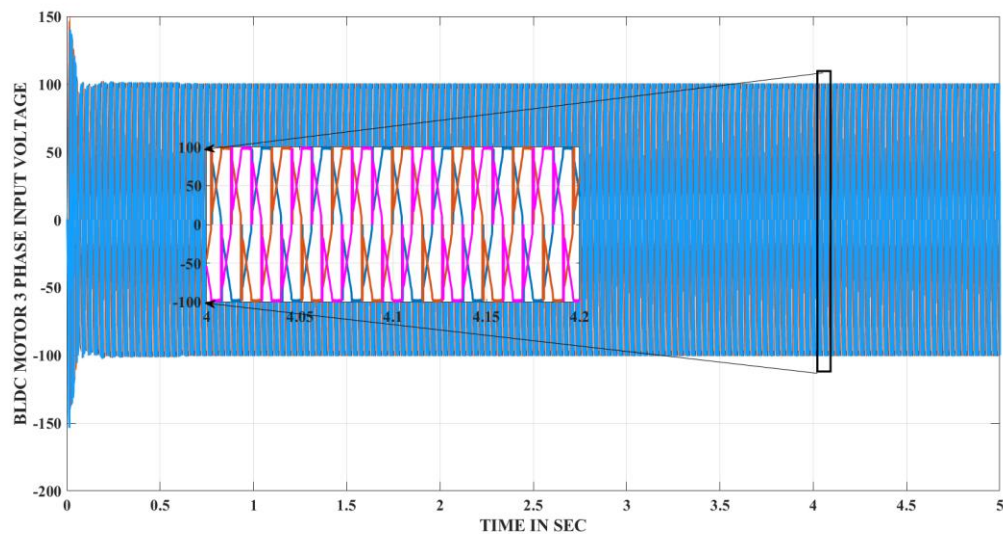


Fig 20: Three Phase BLDC input voltage

Fig 20 the above waveform shows regarding 3 phase input voltage given to the BLDC motor between 0 to 5 seconds time interval. The magnitude of input voltage of each phase is predominantly at 100V i.e., these currents are altering between -100 to +100 Volts. This voltage reached to steady state in less than 0.25 seconds.

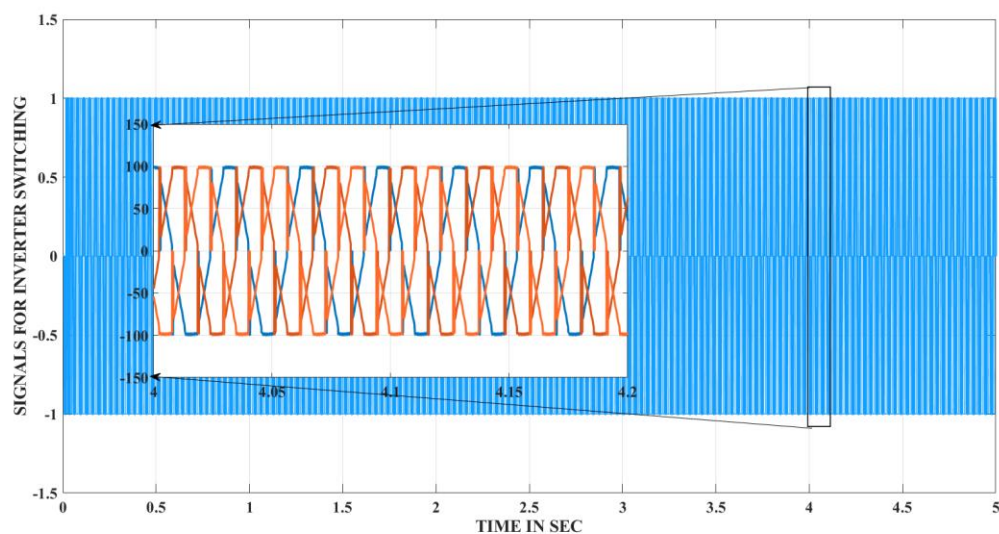


Fig 21: Signals for BLDC Switching

Fig 21 the above waveform shows regarding signals for the inverter switching to the BLDC motor between 0 to 5 seconds time interval. The magnitude of signals for the inverter switching of each is predominantly at 1 i.e., these currents are altering between -1 to +1. These signals reached to steady state in less than 0.25 seconds.

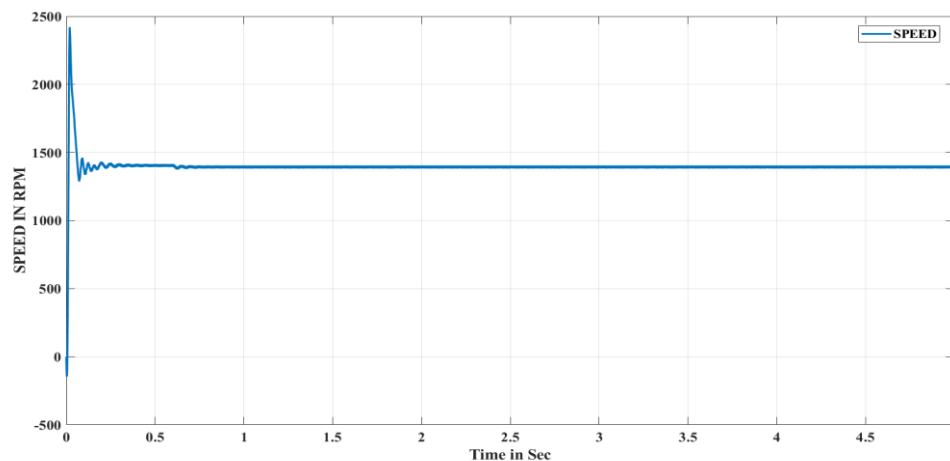


Fig 22: BLDC Motor Speed

Fig 22 the above waveform shows regarding speed to the BLDC motor between 0 to 5 seconds time interval. The RPM of the motor reached around 1400. These signals reached to steady state in less than 0.5 seconds.

7. Conclusion



In this work the DSMST converter is connected to the BLDC motor through a three-phase voltage source inverter (VSI) to regulate the voltage and current supplied to the BLDC motor which shows optimal performance and to regulate the speed of the drive, a closed loop control system is developed using hall sensor signals. The proposed system is developed in the MATLAB/Simulink to check the applicability of electric vehicle configuration and the results shown that the proposed converter is well suitable for electric vehicle applications.

References





- [1] Chan, CC 1993, 'An overview of electric vehicle technology', in Proceedings of the IEEE, vol. 81, no. pp. 1202- 1213.
- [2] Chan, CC 2007, 'The state of the art of electric, hybrid, and fuel cell vehicles', in Proceedings of the IEEE, vol. 95, no. 4, pp. 704-718.
- [3] Bor-Ren Lin & Chung-Wei Chu 2016, 'Hybrid DC–DC converter with high efficiency, wide ZV S range, and less output inductance', International Journal of Circuit Theory and Applications, vol. 44, no. 5, pp. 996-1011
- [4] Tao, H, Duarte, JL & Hendrix, MAM 2008, 'Three-port triple-half-bridge bidirectional converter with zero- voltage switching', IEEE Transactions on Power Electronics, vol. 23, no. 2, pp. 782-792.
- [5] Lai, JS & Nelson, DJ 2007, 'Energy management power converters in hybrid electric and fuel cell vehicles', Proceedings, IEEE, vol. 95, no. 4, pp. 766-777.
- [6] K im, EJ, Cho, CH, K im, W, Lee, CH & Laskar, J 2010, 'Spurious noise reduction by modulating switching frequency in DC-to-DC converter for RF power amplifier', Proceedings of the Symposium on IEEE Radio Frequency Integrated Circuits, pp. 43-46.
- [7] Devikala, S & Nirmalkumar, P 2012, 'Experimental verification of soft switching push-pull DC to DC converter', Proceedings of the IEEE International Conference on Power Electronics, Drives and Energy Systems (PEDES), pp. 1-5.

- [8] Esteki, M, Poorali, B, Adib, E & Farzanehfard, H 2015, 'Interleaved buck converter with continuous input current, extremely low output current ripple, low switching losses, and improved step-down conversion ratio', IEEE Transactions on Industrial Electronics, vol. 62, no. 8, pp. 4769-4776.
- [9] Marchesoni, M & Vaccaro, C 2007, 'New DC-DC converter for energy storage system interfacing in fuel cell hybrid electric vehicles', IEEE Transactions on Power Electronics, vol. 22, no. 1, pp. 301-308.
- [10] Pillay, P & Krishnan, R 1991, 'Application characteristics of permanent magnet synchronous and brushless DC motors for servo drives', IEEE Transactions on Industry Applications, vol. 27, no. 5, pp. 986-996.
- [11] Kavitha, D & Vivekanandan, C 2015, 'An adjustable speed PFC Buckboost converter fed sensorless BLDC motor', International Journal of Applied Engineering Research, vol. 10, no. 20, pp. 17749-17754.
- [12] Yoon, YH & Kim, JM 2018, 'Precision control of a sensorless PM BLDC motor using PLL control algorithm', Journal of Electrical Engineering, vol. 100, no. 2, pp.1097-1111.
- [13] Abdelsalam, I, Philip Adam, G, Holliday, D & Williams, BW 2016, 'Singlestage ac-dc buck-boost converter for medium-voltage high-power application', IET Renewable Power Generation Journal, vol. 10, no. 2, pp. 184-193.
- [14] Pereira, F & Gomes, L 2017, 'The IOPT-Flow modeling framework applied to power electronics controllers', IEEE Trans. on Industrial Electronics, vol. 64, no. 3, pp. 2363-2372.
- [15] Baiju Antony & Gomathy, S 2017, 'Study on DC-DC CONVERTERS for a PFC BLDC motor drive', IOSR Journal of Electrical and Electronics Engineering, pp. 81-88.
- [16] Bist, V & Singh, B 2014, 'An adjustable-speed PFC bridgeless buck-boost converter-fed BLDC motor drive', IEEE Transactions on Industrial Electronics, vol. 61, no. 6, pp. 2665-2677.
- [17] Chen, J, Maksimovic, D & Erickson, RW 2006, 'Analysis and design of a low-stress buck-boost converter in universal-input PFC applications', IEEE Transactions on Power Electronics, vol. 21, no. 2, pp. 320-329.
- [18] B. Das, S. Chakraborty, P. M. Kasari, A. Chakraborti and M. Bhowmik, "Speed control of BLDC Motor using soft computing Technique and its stability analysis," vol. 3, issue 5, ISSN(Online):2249-071X.
- [19] T. Kenjo, "Permanent magnet and brushless dc motor", Oxford, 1985.



¹**Jeetender Vemula**,   received the bachelor's and master's degrees in electrical engineering from Jawaharlal Nehru Technological University, Hyderabad in VBIT and AURB respectively. He is research scholar at Electrical Engineering Department in University college of Engineering, Osmania University, Hyderabad, Telangana.



²**Prof. E. Vidya Sagar**     is currently working as Professor in Electrical Engineering Department, University college of engineering, Osmania University. He has done his bachelor's, master's degree and Doctorate Degree in Engineering from JNTUH college of Engineering Hyderabad. His main research area is Distribution Reliability, Power Quality, Deregulated Power Systems, and Distribution systems. He can be contacted at email: vidyasagar.e@uceou.edu , ORCID ID: <https://orcid.org/0009-0006-5280-7895>.